Water Science & Technology

Water Science & Technology Vol 87 No 11, 2944 doi: 10.2166/wst.2023.178

Combining phthalimide innate of a positive-charge nanofiltration membrane for high selectivity and rejection for bivalent cations

Zhe Wang [a], Jiawei Cao[a], Fan Zhang[a], Xinbo Zhang[a,*] and Xinai Tan[b]

[a] Joint Research Center for Protective Infrastructure Technology and Environmental Green Bioprocess, School of Environmental and Municipal Engineering, Tianjin Chengjian University, Tianjin 300384, China
[b] Dayu Environmental Protection Co., Ltd, Tianjin 301739, China
*Corresponding author. E-mail: zxbcj2006@126.com

ZW, 0000-0001-9573-4258

ABSTRACT

A positively charged nanofiltration (NF) membrane is known to have exceptional separation performance for bivalent cations in aqueous solutions. In this study, a new NF activity layer was created using interfacial polymerization (IP) on a polysulfone (PSF) ultrafiltration substrate membrane. The aqueous phase combines the two monomers of polyethyleneimine (PEI) and phthalimide, while successfully producing a highly efficient and accurate NF membrane. The conditions of the NF membrane were studied and further optimized. The aqueous phase crosslinking process enhances the polymer interaction, resulting in an excellent pure water flux of 7.09 $L{\cdot}m^{-2}{\cdot}h^{-1}{\cdot}bar^{-1}$ under a pressure of 0.4 MPa. Additionally, the NF membrane shows excellent selectivity toward inorganic salts, with a rejection order of $MgCl_2 > CaCl_2 > MgSO_4 > Na_2SO_4 > NaCl$. Under optimal conditions, the membrane was able to reject up to 94.33% of 1,000 mg/L of $MgCl_2$ solution at an ambient temperature. Further to assess the antifouling properties of the membrane with bovine serum albumin (BSA), the flux recovery ratio (FRR) was calculated to be 81.64% after 6 h of filtration. This paper presents an efficient and straightforward approach to customize a positively charged NF membrane. We achieve this by introducing phthalimide, which enhances the membrane's stability and rejection performance.

Key words: interfacial polymerization, nanofiltration membrane, phthalimide, polyethyleneimine, positive charged

HIGHLIGHTS

- A new positive-charge NF membrane was created for the separation of bivalent cations.
- The composite NF membrane demonstrated excellent selectivity and permeability.
- The composite NF membrane exhibited steady antifouling properties.

GRAPHICAL ABSTRACT

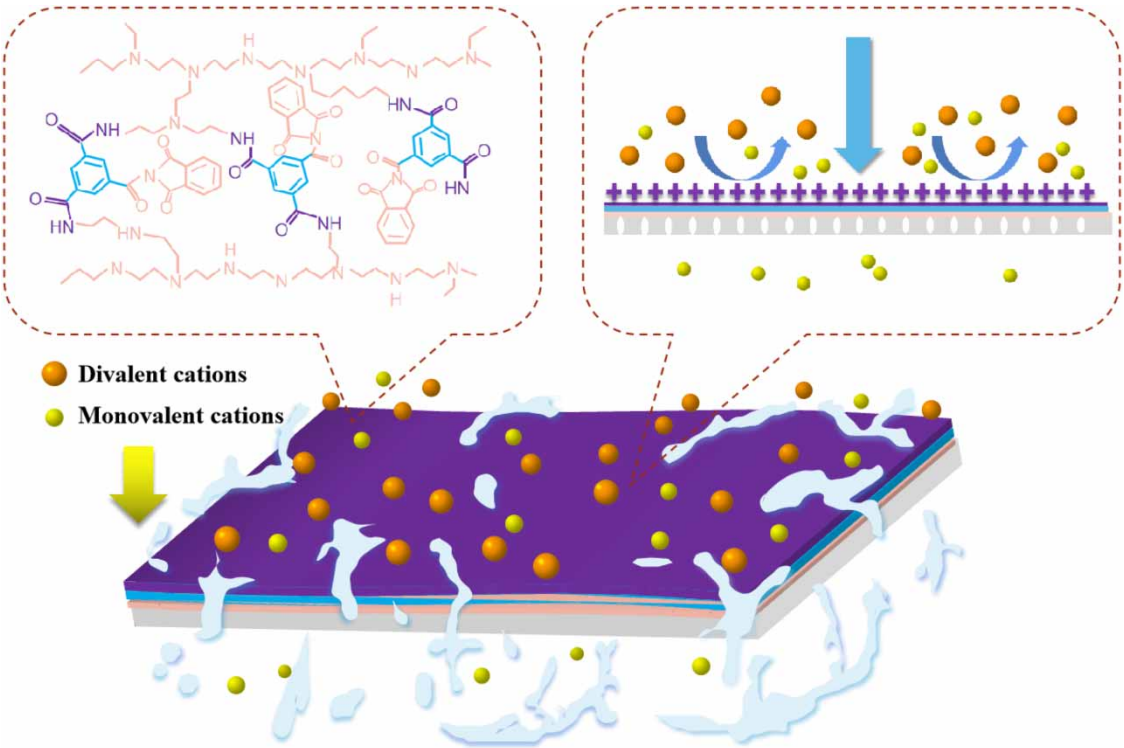

INTRODUCTION

As industries have rapidly developed, the consumption of water resources has increased. However, this has led to the production of effluents containing harmful substances such as dyes, high salinity, and various heavy metals, posing a significant risk to both humans and animals (Zeng *et al.* 2016). To address this issue, nanofiltration (NF) membranes as pressure-driven membranes have been widely used in water treatment processes with a pore diameter range of 0.5–2 nm, allowing them to effectively separate small molecular weight contaminants (Mw = 200–1,000 Da) with high selectivity and low energy consumption (Abdel-Fatah 2018; Qi *et al.* 2019; Wang *et al.* 2021). The NF membrane typically features a function layer that is predominantly negatively charged or neutral, and it operates through a distinctive separation mechanism involving both size sieving and charge repulsion (Chau *et al.* 2021). Currently, the most common functional layers of commercialized NF membranes are thin film composite (TFC), which is a relatively thin and loose polyamide (PA) separation layer fabricated by interfacial polymerization (IP) or crosslinking with amine monomers and acyl chloride. This facilely forms a negatively charged surface due to the unreacted acyl chloride group producing numerous carboxyl groups with deprotonation ability (Ibrahim *et al.* 2020; Zuo *et al.* 2021). The negatively charged NF membrane has a high rejection rate for bivalent anions, and the separation of bivalent cations is to a certain extent unsatisfactory. Hence, developing a positively charged NF membrane is imperative (Kang *et al.* 2021).

Polyethyleneimine (PEI) has massive reactive amine groups, good hydrophilicity, high charge density, and protonated groups, which makes it widely used to prepare a positively charged NF membrane due to the Donnan exclusion principle playing a critical role. Thus, several strategies have been used to obtain the PEI-based positively charged NF membrane. Hoang *et al.* increased the membrane surface area and improved hydrophilicity by incorporating cellulose nanoparticles into the surface of the PEI-TMC NF membrane (Hoang *et al.* 2020). Li *et al.* used 1,2,3,4-cyclobutanetetracarboxylic acid chloride monomer to react with PEI to prepare a positively charged NF membrane, which had a retention rate of 97.53% for $MgCl_2$ and a pure water flux of 156.85 $kg{\cdot}m^{-2}{\cdot}h^{-1}$ (Li *et al.* 2022). Chiang *et al.* prepared a positively charged NF membrane using hyperbranched polyethyleneimine (HPEI) with trimesoyl chloride (TMC) and terephthaloyl chloride (TPC) by IP on the polyacrylonitrile (PAN) surface. The composite membrane exhibited significant rejection for $MgCl_2$ and $MgSO_4$

(Chiang *et al.* 2009). Lehi *et al.* synthesized a highly selective positively charged NF membrane by IP of PEI and TPC, which was further quaternized to increase the membrane separation performance (Lehi *et al.* 2015). It is precise because of the formation of amide groups that the relatively complex preparation process has greatly restricted its development.

In order to increase the NF membrane selectivity, permeability, and stability, it has been found further to adjust the PA layer structure on the membrane surface and improve the membrane surface crosslinking and quaternization, which enhances the NF membrane properties (Xie *et al.* 2012; Zeng *et al.* 2018; Li *et al.* 2019; Cheng *et al.* 2020). Aburabie *et al.* prepared an NF film using rigid brominated stilbene (Tr-X) as a crosslinking agent, which had a water permeability of 7.7 and a retention rate of 99% for dyes (Aburabie *et al.* 2017). Zhu *et al.* used hyperbranched polyacrylonitrile (HPAN) ultrafiltration membrane as the base membrane and added a positively charged quaternary amination crosslinked microgel (PNI6) to form an NF membrane with PNI6 microgel interlayer, which formed a membrane with excellent water flux and a retention rate of 93.4% for $MgCl_2$ (Zhu *et al.* 2023). In this paper, phthalimide as an additive was introduced to the membrane surface to improve the degree of quaternization, and for more amide bonds to form a network of hydrogen bonds. In addition, directly blending the phthalimide into the incorporated PEI aqueous phase solution as the reactive monomer greatly improves the density of positive charge on the membrane surface and simplifies the preparation process. The effects of parameters (including the monomer concentration, reaction time, and temperature) on NF membrane preparation were systematically studied. The NF membrane's chemical properties, morphology, surface charge, and separation performance were characterized and evaluated. Meanwhile, the salt retention rate and antifouling performance of the NF membrane were established in detail.

EXPERIMENT

Materials

Polysulfone (PSF) ultrafiltration membrane as the substrate was obtained from Vontron Technology, Ltd (Guiyang, China). PEI (Mn = 70,000 g mol^{-1}) was purchased from Energy Chemical (Shanghai, China). The organic phase active monomer TMC (98%), the organic solvent n-heptane (AR, >98%), and the aqueous phase monomer additive of phthalimide (AR, > 98%) were obtained from Macklin Biochemical Technology Co. Ltd (Shanghai, China). Sodium chloride (NaCl, AR, >99.5%), anhydrous sodium sulfate (Na_2SO_4, AR, >99%), anhydrous calcium chloride ($CaCl_2$, AR, >96%), magnesium chloride anhydrous ($MgCl_2$, >98%), and magnesium sulfate ($MgSO_4$, AR, >99%) were purchased from Aladdin Reagent Company (Shanghai, China). Bovine serum albumin (BSA, >98%) was purchased from Sigma-Aldrich. Deionized (DI) water was produced by Millipore Milli-Q Advantage A10 (Billeerica, MA, USA). All these chemicals were used without further purification.

Fabrication of the NF membrane

The positively charged composite NF membrane with an active layer of PA/PSF was fabricated via IP. The preparation procedure of the PA/PSF composite NF membrane is briefly illustrated in Figure 1. Firstly, the PSF ultrafiltration membrane was,

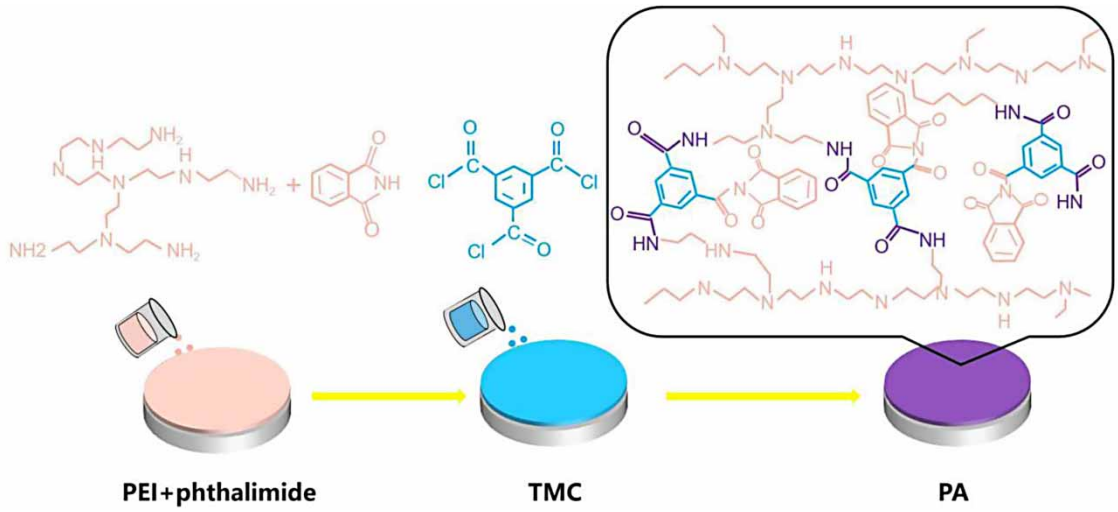

Figure 1 | The preparation route of positively charged NF membrane.

respectively, soaked in the ethanol solution and DI water for removing contaminants before preparation and dried in a vacuum oven. Secondly, a certain ratio of PEI/phthalimide (0.5–1.5 wt%) was dissolved into DI water and the resulting mixture of an aqueous solution was guided and poured onto the surface of the PSF membrane and kept for 1 min. Then, the excess aqueous solution was poured out and the residual solution was removed with a rubber roller. Thirdly, 0.1 wt% of TMC was dissolved into n-heptane solvent as the organic phase, and the as-soaked PEI/phthalimide membrane was immersed in the TMC solution for a certain time and placed in a drying oven at different temperatures for a period of time for further crosslinking. Finally, after the IP reaction, the obtained composite NF membrane was rinsed with DI water and stored for further use. For the control experiments, the NF membrane was prepared in the same way as previously described. The prepared PEI/phthalimide composite NF membranes were labeled as M_1–M_{15} according to the preparation conditions, as listed in Table 1.

The membrane morphology of the surface and cross-section was inspected by scanning electron microscopy (SEM, TESCAN MIRA LMS, Czech Republic). The membrane chemical structure and surface elemental composition were characterized by X-ray photoelectron spectroscopy (XPS, FEI Co., Ltd, USA) with a monochromatic Al Ka X-ray source (1,486.6 eV photons) at a pass energy of 93.9 eV. The membrane surface zeta potential with a streaming potential method was obtained by a Surpass Electrokinetic Analyser (Anton Paar, GmbH, Austria). This measurement was performed in 1 mM KCl background solution at 20 °C. The pH values of the solution ranged from 2 to 10 and adjusted by 0.1 M HCl or 0.1 M NaOH. The zeta potential was calculated using the Helmholtz–Smoluchowski equation.

Membrane filtration performance

The NF membrane permeation and separation performance were evaluated using a cross-flow filtration device at room temperature. Each membrane was compacted to ensure conditional stability under a pressure of 0.4 MPa for 30 min prior to permeation testing with DI water. Then, the salt solutions ($CaCl_2$, $MgCl_2$, $MgSO_4$, NaCl, Na_2SO_4) were performed at 0.4 MPa. All measurements were executed three times to obtain the average value and guarantee the reproducibility of the test results. The flux (J) and salt rejection (R) were calculated by the following equations, respectively (Li *et al.* 2014).

$$J = \frac{V}{At} \tag{1}$$

$$R = \left(1 - \frac{C_p}{C_f}\right) \times 100\% \tag{2}$$

Table 1 | Preparation of composite NF membranes

Membranes	PEI concentration (wt%)	Phthalimide concentration (wt%)	TMC concentration (wt%)	IP time (min)	IP temperature (°C)
M_1	0.5	/	0.1	10	75
M_2	1.0	/	0.1	10	75
M_3	1.5	/	0.1	10	75
M_4	0.5	0.1	0.1	10	75
M_5	1.0	0.1	0.1	10	75
M_6	1.5	0.1	0.1	10	75
M_7	1.0	0.05	0.1	10	75
M_8	1.0	0.15	0.1	10	75
M_9	1.0	0.1	0.1	5	75
M_{10}	1.0	0.1	0.1	15	75
M_{11}	1.0	0.1	0.1	20	75
M_{12}	1.0	0.1	0.1	10	55
M_{13}	1.0	0.1	0.1	10	65
M_{14}	1.0	0.1	0.1	10	85
M_{15}	1.0	0.1	0.1	10	95

where J is the permeation flux ($L{\cdot}m^{-2}{\cdot}h^{-1}{\cdot}bar^{-1}$), V is the permeation volume (L), t is the collection time (h), A is the effective membrane area (m^2), C_f and C_p are the concentrations of the salt solutions in feed and permeation solutions, respectively.

Antifouling performance of an NF membrane

In this experiment, the membrane fouling was examined by 1 g/L of BSA as a simulated pollutant. During the filtration experiments, a cross-flow filtration device was used to provide vigorous mixing at room temperature in order to reduce concentration polarization on the membrane surface (Wang *et al.* 2019; Yang *et al.* 2021). Several indicators were used to quantitatively evaluate the anti-pollution performance of the membrane, including flux decay rate (DR_t), reversible flux decay rate (DR_r), irreversible flux decay rate (DR_{ir}), and flux recovery ratio (FRR). These parameters were calculated from the following equations (Chen *et al.* 2015; Zeng *et al.* 2018).

$$DR_t = \frac{J_0 - J_t}{J_0} \times 100\% \tag{3}$$

$$DR_r = \frac{J_r - J_t}{J_0} \times 100\% \tag{4}$$

$$DR_{ir} = \frac{J_0 - J_r}{J_0} \times 100\% \tag{5}$$

$$FRR = \frac{J_r}{J_0} \times 100\% \tag{6}$$

where J_0 is the average pure water flux, J_t is the average flux in contamination, and J_r is the average flux after cleaning. The filtration and washing cycles were repeated for 3 times.

RESULTS AND DISCUSSION

Characterization of membranes

The morphology of the original membrane and the positively charged modified NF membrane were visualized by SEM to observe the cross-sectional and surface images as shown in Figure 2. It can be observed that the pristine PSF membrane

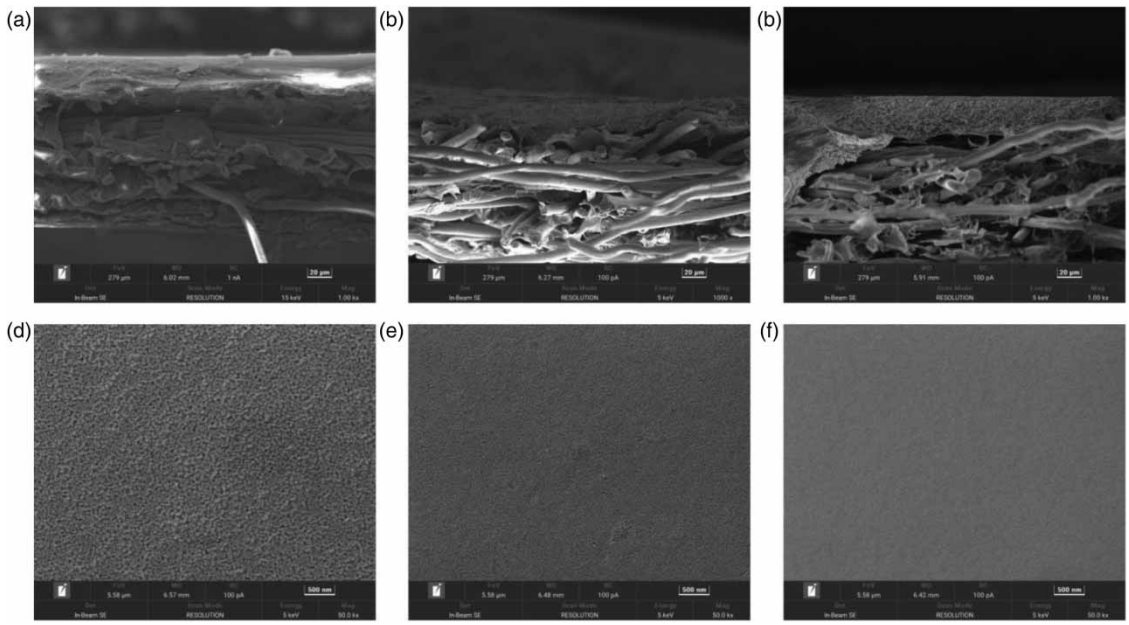

Figure 2 | The cross-sectional (×1K) morphology and surface (×50 K) morphology of original membrane and NF membranes (a and d indicate the original membrane, b and e indicate M_2, c and f indicate M_5).

presented a loose surface morphology and a typical macrovoid structure (Figure 2(a)), with no visible separation layer on the surface of the membrane (Figure 2(d)). The membrane surface was obviously covered with a compact layer after the IP reaction, and the M_5 membrane (Figure 2(e)) displayed a more uniform and denser surface by introducing phthalimide as the co-aqueous phase. It was confirmed that the NF active layer was formed onto the PSF substrate. In addition, the active layer thickness of the M_5 membrane (Figure 2(c)) increased slightly compared to the M_2 membrane (Figure 2(b)), which revealed that the M_5 had a higher degree of crosslinking. These results indicated that the NF active layer was successfully fabricated on the PSF substrate membrane.

The surface chemical compositions of the membranes were analyzed by XPS (Li *et al.* 2022). As seen in Figure 3(a) and Table 2, the original membrane did not contain element N; however, it was present in both M_2 and M_5. This indicates that an IP reaction between PEI and TMC occurred on the surface of the PSF membrane to form a PA layer. Compared with the M_2 membrane, the N element on the membrane surface of M_5 increased from 0.7 to 12.3%, while the content of O element decreased from 9.4 to 6.1%. It was due to the large amount of N element in the phthalimide added in the aqueous phase during the preparation of M_5, and the phthalimide participated in the IP reaction at the same time to optimize the structure of the membrane surface. To further investigate the chemical composition in the PA layer on the membrane surface, the N spectrum of M_5 was divided and the results are shown in Figure 3(b). It can be seen that the characteristic peak of O = C–NH– appears at the electron binding energy of 399.7 eV, which proves that the IP reaction occurred on the surface of the PSF membrane and the amide bond was formed (Zarshenas *et al.* 2021; Xu *et al.* 2022). The characteristic peaks of C–N at the electron binding energy 396.9 eV and C–N^+ at the electron binding energy 401.6 eV prove that the membrane surface is positively charged.

The NF membrane surface charge affects the selectivity and rejection of bivalent cations in water treatment processes in accordance with the Donnan effect (Shen *et al.* 2020; Zhang *et al.* 2021a, 2021b). The streaming potential measurement determined the charge properties of the membrane surface. As shown in Figure 4, the PSF original membrane had a negative charge with a wide pH range, and the isoelectric point was presented at an approximate pH of 4.2, which was an intrinsic

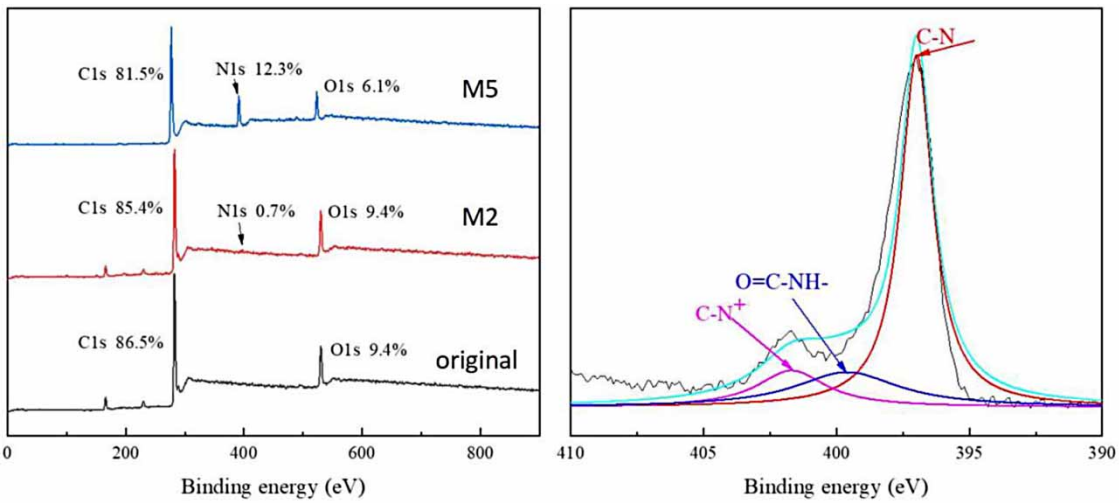

Figure 3 | Wide-scan XPS spectra of NF composite and original membranes (a) and XPS N1s spectra of M_5 (b).

Table 2 | The surface chemical compositions of the original and NF membranes

Membranes	C (wt%)	O (wt%)	N (wt%)	O/C	O/N
Original	86.50	9.40		0.11	
M_2	85.40	9.40	0.70	0.11	13.43
M_5	81.50	6.10	12.3	0.07	0.50

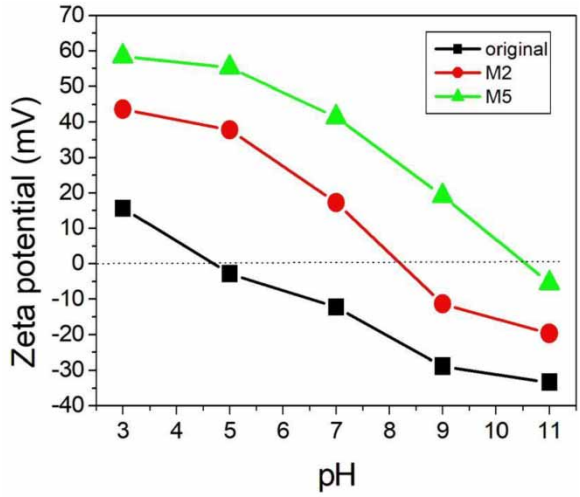

Figure 4 | The surface potential of the original membrane and NF membrane (M_2 and M_5).

property of the polymer membrane that would adsorb the anions such as hydroxide (Feng *et al.* 2022). The isoelectric point of the obtained NF membrane with only PEI as the aqueous phase (M_2) was at pH = 8.1. However, with the introduction of phthalimide as the mixing aqueous phase, the NF membrane (M_5) isoelectric point increased to 10.2. It indicated that the mixing of the aqueous phase obtained NF membrane with a more strong positive charge, which further demonstrated that the phthalimide was successfully incorporated on the membrane by IP reaction.

Effect of fabrication condition on the pure water flux and rejection of the NF membrane

The preparation conditions are very important for affecting the NF membrane rejection and permeation performance (Ma *et al.* 2016; Fang *et al.* 2019). Firstly, only PEI as the aqueous phase was selected to prepare the NF membrane by IP reaction with 0.1 wt% TMC at 75 °C for 10 min. As shown in Figure 5(a), the results indicated that the pure water flux decreased with the increase in the PEI concentration, while the $MgCl_2$ rejection gradually increased with the increase in the PEI concentration. Although the rejection rate of the NF membrane presented a maximum value when the PEI content reached up to 1 wt%, the permeation flux was about 2.13 $L{\cdot}m^{-2}{\cdot}h^{-1}{\cdot}bar^{-1}$. Subsequently, there was little effect on the NF membrane rejection performance with excess PEI concentration. It was speculated that the NF membrane separating process was chiefly affected by the steric hindrance effect because of the loose PA layer formed (Xu *et al.* 2019).

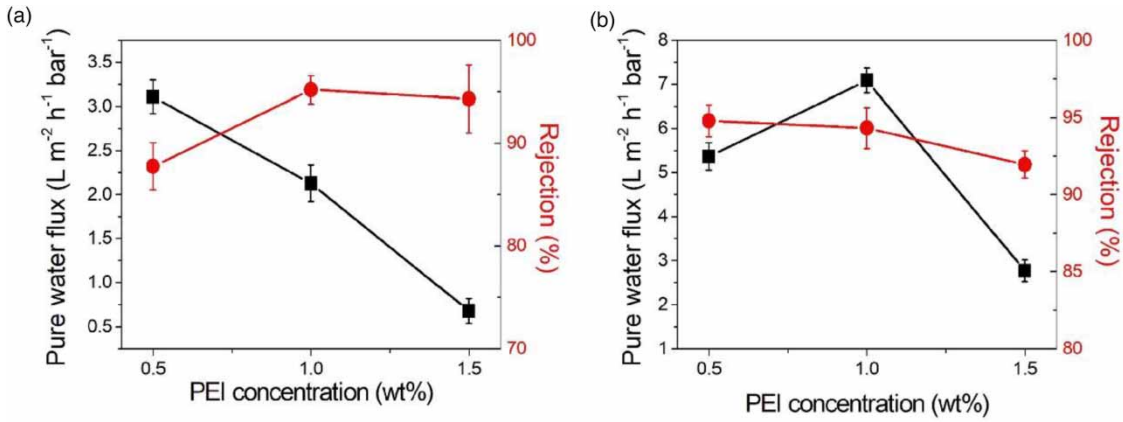

Figure 5 | Effect of PEI concentrations on NF membrane performance of rejection and flux. (a) Only PEI is present in the aqueous phase, (b) PEI and phthalimide are both used as aqueous phases.

The NF membrane permeate flux improved noticeably when 0.1 wt% of phthalimide was added to the aqueous phase compared with when PEI was added under the same conditions. Figure 5(b) shows the effect of PEI concentration on the pure water flux and $MgCl_2$ rejection from 0.5 to 1.5 wt%. It was found that the permeation flux of the NF membrane was significantly increased and the maximum value achieved 7.09 $L{\cdot}m^{-2}{\cdot}h^{-1}{\cdot}bar^{-1}$ after adding the phthalimide, which was more than twice better than that of the NF membrane without adding phthalimide. In addition, the rejection rate remained at high levels. It could be attributed to the mixed amino group leading to the functional layer having a high crosslinking density, and phthalimide was introduced to enhance the hydrophilicity and contributed to increasing the positive charge density of the NF membrane surface. However, further increasing the concentration of PEI could lead to a reduction in the NF membrane's separating property.

The phthalimide concentration of the aqueous phase was further researched in relation to the pure water flux and $MgCl_2$ rejection of the NF membrane, and the results are shown in Figure 6. It was observed that the pure water flux increased rapidly and the rejection declined gradually with an increase in the phthalimide concentration. This was due to the elevation of the phthalimide concentration with loading amount of the amino to promote the hydrophilicity on the membrane surface. In turn, the NF separation layer became thicker and denser after the phthalimide concentration was increased, which led to a decrease in the rejection. When the phthalimide concentration was increased to 0.1 wt%, the $MgCl_2$ rejection remained at a high state and the pure water flux achieved a better level. Therefore, 0.1 wt% was used as the appreciated phthalimide concentration in the aqueous phase to prepare the NF membrane.

The IP reaction time is an important preparation parameter that affects the NF membrane performance of water flux and rejection (Lu & Elimelech 2021). Figure 7 shows the IP reaction time in the range of 5–20 min on the $MgCl_2$ rejection and pure water flux under the condition of immersion in 0.1 wt% phthalimide and 1 wt% PEI aqueous solution with 0.1 wt% TMC at 75 °C. The results indicated that the pure water flux decreased sharply and the rejection increased first and then remained stable with increasing IP reaction time. Obviously, the denser and more compact active layer was formed when the IP reaction time was prolonged further. However, a short reaction time will lead to an incomplete IP reaction process (Wu *et al.* 2015). Thus, when the IP was almost finished in 10 min, the $MgCl_2$ rejection was 94.33%, and the pure water flux was 7.09 $L{\cdot}m^{-2}{\cdot}h^{-1}{\cdot}bar^{-1}$.

The post-heat treatment is another important factor that affects the NF membrane rejection and flux, as it has a potential role in removing excess organic solvent and accelerating the amidation crosslinking rate with amine and acyl chloride (Ouyang *et al.* 2019; Soyekwo *et al.* 2022). Figure 8 shows the effect of heat curing temperature from 55 to 95 °C on the NF membrane flux and separation performances. The results show that the pure water flux decreases while the $MgCl_2$ rejection increases with increased crosslinking temperature before 75 °C. However, the opposite result of NF membrane performances occurs after 75 °C. It was revealed that the post-heat treatment accelerates the degree of crosslinking in the IP reaction. However, a high crosslinking of degree will enhance the compactness of the NF membrane surface and lead to a shrinkage of the pore structure. A low degree of crosslinking will form a loose structure of the membrane surface,

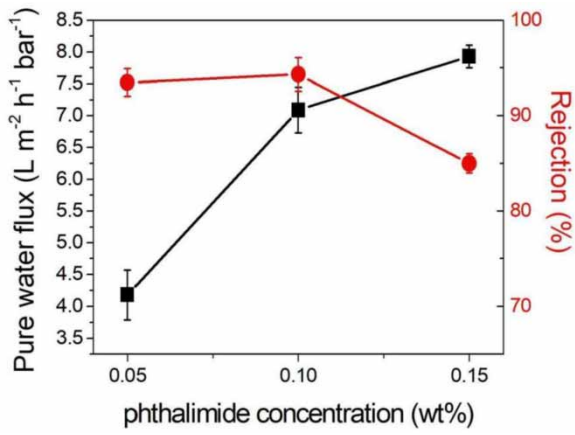

Figure 6 | Effect of the phthalimide concentration in the aqueous phase during membrane performance.

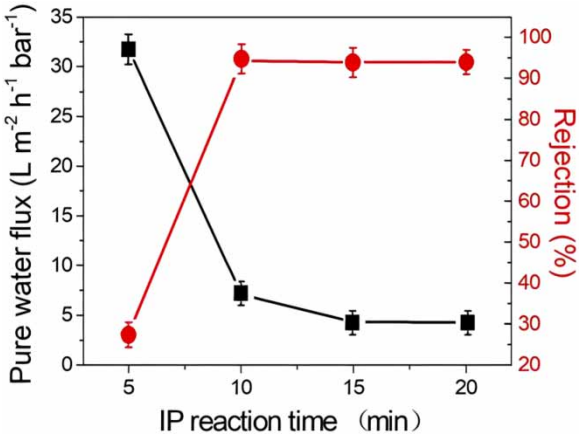

Figure 7 | Effect of IP reaction times on the NF membrane flux and rejection performances.

resulting in an increase in pore size (Li *et al.* 2014). Thus, the optimized conditions of post-heat treatment temperature for NF membrane fabrication are 75 °C with 10 min.

Salt separation performance of membranes

The salt rejection of the M5 NF membrane mainly depends on the electrostatic repulsion rather than the size sieving. This is because the salt ions' hydrodynamic radius is far less than the membrane pore radius (Shao *et al.* 2022). The NF membrane rejection performance was further studied with a different inorganic salt, and the results are shown in Figure 9. It was indicated that the rejection order was $MgCl_2 > CaCl_2 > MgSO_4 > Na_2SO_4 > NaCl$, exhibiting the typical rejection characteristic of positively charged NF membranes. According to the Donnan exclusion theory and the steric hindrance effect, it is undoubted that there is lower rejection for sulfates and largely rejection for chlorine salts (Chen *et al.* 2015). However, the monovalent ions of NaCl have a small hydrated radius, a high diffusion coefficient, and weaker electrostatic repulsive interaction, leading to the lowest rejection. In addition, the ionic hydration radius and ion diffusion coefficient are shown in Table 3. In short, high valence cations with more positive charges contribute to improving repulsive interaction between the cation and NF membrane. Conversely, the stronger negative charge of high valence anions is more likely to attract the NF membrane.

Antifouling properties of membranes

BSA has been frequently used as a model sticky protein pollutant to measure the non-specific adsorption of NF membranes in the water treatment fouling process. For a typical cross-flow filtration in this study, BSA was used as a foulant to estimate the

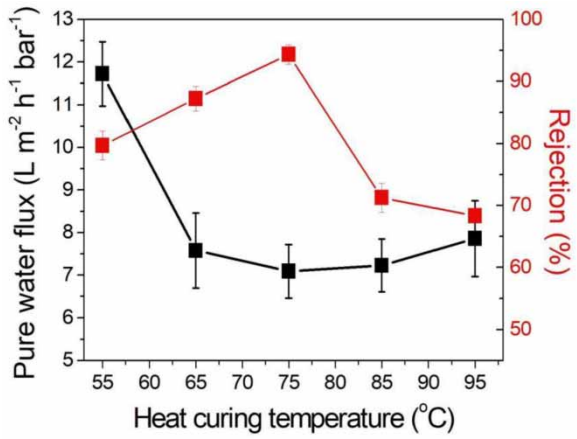

Figure 8 | Effect of the reaction temperature on the performance of the NF membrane.

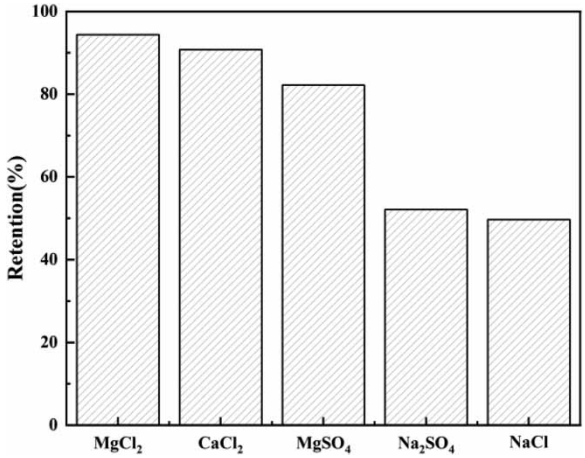

Figure 9 | NF membrane separation and rejection performance for different inorganic salts.

Table 3 | Ionic hydration radius and diffusion coefficient

Ionic species	Ionic hydration radius (nm)	Diffusion coefficient (10^{-9}·m^2·s^{-1})
Mg^{2+}	0.35	0.70
SO_4^{2-}	0.23	1.06
Na^{+}	0.18	1.33
Cl^{-}	0.12	2.01

antifouling properties of M5 NF membrane and the results after three cycles are shown in Figure 10. It can be seen that the permeation flux of the NF membrane inevitably reduces through the BSA solution (Zhang *et al.* 2021a, 2021b; Wang *et al.* 2022). After three cycles with pure water and BSA alternate filtration, the flux of NF lowered from 7.09 [1] to 5.78 L·m^{-2}·h^{-1}·bar^{-1}. Meanwhile, the FRR values gradually declined. This was due to the cake layer formation by persistent protein pollution. Even so, the FRR value of the NF membrane still exceeded 81.64% in the whole filtration process. The presence of PEI and phthalimide mixing amino groups increased the positively charge density of membrane surface and formed a hydrophilic hydrogel layer.

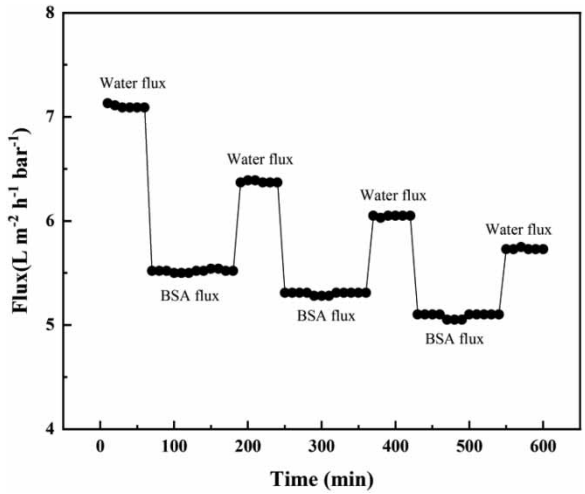

Figure 10 | The time-dependent pure water flux and BSA rejection of the NF membrane.

CONCLUSION

In this work, the positively charged NF membrane was successfully fabricated by introducing phthalimide as a co-aqueous phase with PEI via an IP reaction process. The optimized NF membrane revealed higher inorganic salt rejection and pure water permeation flux. In addition, antifouling properties and durability of the NF membrane were significantly improved. This study offered an effective method to obtain a convenient fabrication process to synthesize positively charged NF membrane with high stability and rejection performance for separating the multivalent cations.

ACKNOWLEDGEMENTS

This research was supported by the Research Project of the Tianjin Education Commission (No. 2019KJ097).

DATA AVAILABILITY STATEMENT

All relevant data are included in the paper or its Supplementary Information.

CONFLICT OF INTEREST

The authors declare there is no conflict.

REFERENCES

Abdel-Fatah, M. A. 2018 Nanofiltration systems and applications in wastewater treatment. *Ain Shams Eng. J.* **9**, 3077–3092. http//dx.doi.org/10.1016/j.asej.2018.08.001.

Aburabie, J., Villalobos, L. F. & Peinemann, K. V. 2017 Composite membrane formation by combination of reaction-induced and nonsolvent-induced phase separation. *Macromol. Mater. Eng.* **302**, 1700131. https//doi.org/10.1002/mame.201700131.

Chau, J., Sirkar, K. K., Pennisi, K. J., Vaseghi, G., Derdour, L. & Cohen, B. 2021 Novel perfluorinated nanofiltration membranes for isolation of pharmaceutical compounds. *Sep. Purif. Technol.* **258**, 117944. https//doi.org/10.1016/j.seppur.2020.117944.

Chen, Q., Yu, P., Huang, W., Yu, S., Liu, M. & Gao, C. 2015 High-flux composite hollow fiber nanofiltration membranes fabricated through layer-by-layer deposition of oppositely charged crosslinked polyelectrolytes for dye removal. *J. Membr. Sci.* **492**, 312–321. https//doi.org/10.1016/j.memsci.2015.05.068.

Cheng, X., Pan, Q., Liu, T., Tan, H. & Liu, W. 2020 Manipulating the separation performance of nanofiltration membranes by coating thickness of organic phase during interfacial polymerization. *J. Appl. Polym. Sci.* **137**, 48284. http//dx.doi.org/10.1002/app.48284.

Chiang, Y. C., Hsub, Y. Z., Ruaan, R. C., Chuang, C. J. & Tung, K. L. 2009 Nanofiltration membranes synthesized from hyperbranched polyethyleneimine. *J. Membr. Sci.* **326**, 19–26. https//doi.org/10.1016/j.memsci.2008.09.021.

Fang, L. F., Zhou, M. Y., Cheng, L., Zhu, B. K., Matsuyama, H. & Zhao, S. 2019 Positively charged nanofiltration membrane based on cross-linked polyvinyl chloride copolymer. *J. Membr. Sci.* **572**, 28–37. http//dx.doi.org/10.1016/j.memsci.2018.10.054.

Feng, Y., Peng, H. & Zhao, Q. 2022 Fabrication of high performance Mg^{2+}/Li^{+} nanofiltration membranes by surface grafting of quaternized bipyridine. *Sep. Purif. Technol.* **280**, 119848. https//doi.org/10.1016/j.seppur.2021.119848.

Hoang, M. T., Pham, T. D., Verheyen, D., Nguyen, M. K., Pham, T. T., Zhu, J. & Van der Bruggen, B. 2020 Fabrication of thin film nanocomposite nanofiltration membrane incorporated with cellulose nanocrystals for removal of Cu (II) and Pb (II). *Chem. Eng. Sci.* **228**, 115998. https//doi.org/10.1016/j.ces.2020.115998.

Ibrahim, Y., Naddeo, V., Banat, F. & Hasan, S. W. 2020 Preparation of novel polyvinylidene fluoride (PVDF)-Tin(IV) oxide (sno_2) ion exchange mixed matrix membranes for the removal of heavy metals from aqueous solutions. *Sep. Purif. Technol.* **250**, 117250. https//doi.org/10.1016/j.seppur.2020.117250.

Kang, D., Shao, H., Chen, G., Dong, X. & Qin, S. 2021 Fabrication of highly permeable PVDF loose nanofiltration composite membranes for the effective separation of dye/salt mixtures. *J. Membr. Sci.* **621**, 118951. https//doi.org/10.1016/j.memsci.2020.118951.

Lehi, A. Y., Akbari, A. & Soleimani, H. 2015 Preparation of novel NF membrane via interfacial cross-linking polymerization. *Membr. Water Treat.* **6**, 173–187. https//doi.org/10.12989/mwt.2015.6.3.173.

Li, Y., Su, Y., Dong, Y., Zhao, X., Jiang, Z., Zhang, R. & Zhao, J. 2014 Separation performance of thin-film composite nanofiltration membrane through interfacial polymerization using different amine monomers. *Desalination* **333**, 59–65. https//doi.org/10.1016/j.desal.2013.11.035.

Li, S. L., Shan, X., Zhao, Y. & Hu, Y. 2019 Fabrication of a novel nanofiltration membrane with enhanced performance via interfacial polymerization through the incorporation of a new zwitterionic diamine monomer. *ACS Appl. Mater. Interfaces* **11**, 42846–42855. https//doi.org/10.1021/acsami.9b15811.

Li, P., Lan, H., Chen, K., Ma, X., Wei, B., Wang, M., Li, P., Hou, Y. & Niu, Q. J. 2022 Novel high-flux positively charged aliphatic polyamide nanofiltration membrane for selective removal of heavy metals. *Sep. Purif. Technol.* **280**, 119949. https//doi.org/10.1016/j.seppur.2021.119949.

Lu, X. & Elimelech, M. 2021 Fabrication of desalination membranes by interfacial polymerization: history, current efforts, and future directions. *Chem. Soc. Rev.* **50**, 6290–6307. https//doi.org/10.1039/D0CS00502A.

Ma, T., Su, Y., Li, Y., Zhang, R., Liu, Y., He, M., Li, Y., Dong, N., Wu, H. & Jiang, Z. 2016 Fabrication of electro-neutral nanofiltration membranes at neutral pH with antifouling surface via interfacial polymerization from a novel zwitterionic amine monomer. *J. Membr. Sci.* **503**, 101–109. https//doi.org/10.1016/j.memsci.2015.12.038.

Ouyang, Z., Huang, Z., Tang, X., Xiong, C., Tang, M. & Lu, Y. 2019 A dually charged nanofiltration membrane by pH-responsive polydopamine for pharmaceuticals and personal care products removal. *Sep. Purif. Technol.* **211**, 90–97. https//doi.org/10.1016/j.seppur.2018.09.059.

Qi, Y., Zhu, L., Shen, X., Sotto, A., Gao, C. & Shen, J. 2019 Polythyleneimine-modified original positive charged nanofiltration membrane: removal of heavy metal ions and dyes. *Sep. Purif. Technol.* **222**, 117–124. https//doi.org/10.1016/j.seppur.2019.03.083.

Shao, S., Zeng, F., Long, L., Zhu, X., Peng, L. E., Wang, F. & Tang, C. Y. 2022 Nanofiltration membranes with crumpled polyamide films: a critical review on mechanisms, performances, and environmental applications. *Environ. Sci. Technol.* **56**, 12811–12827. https//doi.org/10.1021/acs.est.2c04736.

Shen, Q., Xu, S. J., Dong, Z. Q., Zhang, H. Z., Xu, Z. L. & Tang, C. Y. 2020 Polyethyleneimine modified carbohydrate doped thin film composite nanofiltration membrane for purification of drinking water. *J. Membr. Sci.* **610**, 118220. https//doi.org/10.1016/j.memsci.2020.118220.

Soyekwo, F., Wen, H., Liao, D. & Liu, C. 2022 Nanofiltration membranes modified with a clustered multiquaternary ammonium-based ionic liquid for improved magnesium/ lithium separation. *ACS Appl. Mater. Interfaces* **14**, 32420–32432. https//doi.org/10.1021/acsami.2c03650.

Wang, J., Zhang, S., Wu, P., Shi, W., Wang, Z. & Hu, Y. 2019 In situ surface modification of thin-film composite polyamide membrane with zwitterions for enhanced chlorine resistance and transport properties. *ACS Appl. Mater. Interfaces* **11**, 12043–12052. https//doi.org/10.1021/acsami.8b21572.

Wang, Z., Ma, C., Xu, C., Sinquefield, S. A., Shofner, M. L. & Nair, S. 2021 Graphene oxide nanofiltration membranes for desalination under realistic conditions. *Nat. Sustainability* **4**, 402–408. Available from: https//www.x-mol.com/paperRedirect/1351304671795113984

Wang, J., Li, S. L., Guan, Y., Zhu, C., Gong, G. & Hu, Y. 2022 Novel RO membranes fabricated by grafting sulfonamide group: improving water permeability, fouling resistance and chlorine resistant performance. *J. Membr. Sci.* **641**, 119919. https//doi.org/10.1016/j.memsci.2021.119919.

Wu, D., Yu, S., Lawless, D. & Feng, X. 2015 Thin film composite nanofiltration membranes fabricated from polymeric amine polyethylenimine imbedded with monomeric amine piperazine for enhanced salt separations. *React. Funct. Polym.* **86**, 168–183. https//doi.org/10.1016/j.reactfunctpolym.2014.08.009.

Xie, W., Geise, G. M., Freeman, B. D., Lee, H. S., Byun, G. & McGrath, J. E. 2012 Polyamide interfacial composite membranes prepared from m-phenylene diamine, trimesoyl chloride and a new disulfonated diamine. *J. Membr. Sci.* **403**, 152–161. https//doi.org/10.1016/j.memsci.2012.02.038.

Xu, P., Wang, W., Qian, X., Wang, H., Guo, C., Li, N. & Wang, Z. 2019 Positive charged PEI-TMC composite nanofiltration membrane for separation of Li^+ and Mg^{2+} from brine with high Mg^{2+}/Li^+ ratio. *Desalination* **449**, 57–68. https//doi.org/10.1016/j.desal.2018.10.019.

Xu, Y., Peng, H., Luo, H., Zhang, Q., Liu, Z. & Zhao, Q. 2022 High performance Mg^{2+}/Li^+ separation membranes modified by a bis-quaternary ammonium salt. *Desalination* **526**, 115519. https//doi.org/10.1016/j.desal.2021.115519.

Yang, Z., Fang, W., Wang, Z., Zhang, R., Zhu, Y. & Jin, J. 2021 Dual-skin layer nanofiltration membranes for highly selective Li^+/Mg^{2+} separation. *J. Membr. Sci.* **620**, 118862. http//dx.doi.org/10.1016/j.memsci.2020.118862.

Zarshenas, K., Dou, H., Habibpour, S., Yu, A. & Chen, Z. 2021 Thin film polyamide nanocomposite membrane decorated by polyphenol-assisted $Ti_3C_2T_x$ MXene nanosheets for reverse osmosis. *ACS Appl. Mater. Interfaces* **14**, 1838–1849. https//doi.org/10.1021/acsami.1c16229.

Zeng, G., He, Y., Zhan, Y., Zhang, L., Pan, Y., Zhang, C. & Yu, Z. 2016 Novel polyvinylidene fluoride nanofiltration membrane blended with functionalized halloysite nanotubes for dye and heavy metal ions removal. *J. Hazard. Mater.* **317**, 60–72. http//dx.doi.org/10.1155/2018/3849867.

Zeng, Y., Wang, L., Zhang, L. & Yu, J. Q. 2018 An acid resistant nanofiltration membrane prepared from a precursor of poly(s-triazine-amine) by interfacial polymerization. *J. Membr. Sci.* **546**, 225–233. https//doi.org/10.1016/j.memsci.2017.10.022.

Zhang, L., Zhang, R., Ji, M., Lu, Y., Zhu, Y. & Jin, J. 2021a Polyamide nanofiltration membrane with high mono/divalent salt selectivity via pre-diffusion interfacial polymerization. *J. Membr. Sci.* **636**, 119478. http//dx.doi.org/10.1016/j.memsci.2021.119478.

Zhang, X., Chen, T. H., Chen, F. F., Wu, H., Yu, C. Y., Liu, L. F. & Gao, C. J. 2021b Structure adjustment for enhancing the water permeability and separation selectivity of the thin film composite nanofiltration membrane based on a dendritic hyperbranched polymer. *J. Membr. Sci.* **618**, 118455. https//doi.org/10.1016/j.memsci.2020.118455.

Zhu, S., Dong, S., Fan, W., Nie, J., Zhu, L. & Du, B. 2023 Preparation of high-performance nanofiltration membranes with quaternized cross-linked microgels as intermediate layer. *Desalination* **549**, 116310. https//doi.org/10.1016/j.desal.2022.116310.

Zuo, C., Wang, L., Tong, Y., Shi, L., Ding, W. & Li, W. 2021 Co-deposition of pyrogallol/polyethyleneimine on polymer membranes for highly efficient treatment of oil-in-water emulsion. *Sep. Purif. Technol.* **267**, 118660. https//doi.org/10.1016/J.SEPPUR.2021.118660.

First received 23 April 2023; accepted in revised form 25 May 2023. Available online 8 June 2023